

MARGINAL ADAPTABILITY AND FRACTURE RESISTANCE OF ENDODONTICALLY TREATED PREMOLARS RESTORED WITH 3D PRINTED AND MILLED ENDO-CROWNS

Ahmed Mohamed Arafa*^{ID} and Ahmed Ziada**^{ID}

ABSTRACT

Objectives: to evaluate marginal adaptability of root canal treated premolars restored with 3D printed and milled endo-crowns before and after thermo-mechanical aging, fracture resistance, and failure modes.

Materials and methods: Thirty-six mandibular first premolars were endodontically treated and prepared to receive endo-crowns that were divided according to CAD-CAM restorative material used into 3 groups (n=12): 3D printed (Varseo Smile) group, Brilliant Crios (BC) group and PEEK group. Marginal gap was measured before and after thermo-mechanical aging for 60000 loading cycles and 5000 thermocycles. Fracture loads were recorded, and failure modes were evaluated.

Results: Paired t-test revealed significant increase in overall marginal gap rates after thermo-mechanical aging of all tested groups with significant difference among them as verified by One Way ANOVA test. There was a significant difference between fracture resistance mean values of all tested groups ($P < 0.0001$) where insignificant difference between Brilliant Crios (1879.45 ± 477.60 N) and PEEK groups (1730.5 ± 210.56 N) both revealed statistically significantly higher mean fracture resistance than 3D printed group (743.39 ± 68.71 N) as verified by Tukey's Post Hoc test.

Conclusions: Marginal adaptability of PEEK endo-crowns was better than those of Brilliant Crios and 3D printed (VarseoSmile) before and after thermo-mechanical aging which resulted in significant reduction of marginal adaptability of all tested endo-crowns. Fracture resistance of Brilliant Crios endo-crowns was higher than those of PEEK and 3D printed (VarseoSmile). Regarding failure mode, all tested endo-crowns showed repairable (favorable) fractures.

KEYWORDS: 3D printing, CAD-CAM, marginal adaptability, thermo-mechanical aging, fracture resistance, premolar endo-crown.

* Lecturer, Department of Fixed Prosthodontics, Faculty of Dentistry, Beni-Suef University, Beni-Suef, Egypt.

** Associate Professor, Department of Fixed Prosthodontics, Faculty of Dentistry, Beni-Suef University, Beni-Suef, Egypt.

INTRODUCTION

The expected success of the root canal treatment (RCT) is strongly dependent on the ideal restoration protocol which is still a controversial and challenging issue. Excessive loss of tooth tissue together with intense stress under functional forces elevates the risk of fracture⁽¹⁾. The guide during the selection of treatment protocol for such teeth should fulfill the mechanical, functional, and esthetic requirements in addition to obtaining a long-term coronal seal⁽²⁾. The most common approach that has been recommended to restore endodontically treated teeth was intra-radicular post and core with an overlying crown. Although posts, whether prefabricated or custom-made are required to enhance the retention of the core foundation, it may cause weakening of the root⁽¹⁾.

The insertion of metallic posts can increase the opportunity of catastrophic root fracture which might be attributed to the increased rigidity and stiffness causing stress concentration while the fiber-reinforced posts such as glass-fiber, carbon-fiber, and quartz-fiber posts with a modulus of elasticity similar to that of the dentin of the tooth can form a "mono-block" within the root canal for a unified root complex⁽³⁾ but cyclic elastic bending between the crown & core interface will induce micro-gaps, leakage, bacterial infiltration, and subsequent failure of the restoration⁽⁴⁾.

The risk of root fracture⁽⁵⁾ can be reduced by adequate ferrule preparation which is a challenging issue in endodontically treated teeth that are grossly destructed⁽⁶⁾ so, the biochemical deterioration of post and core systems under intra-oral cyclic stresses may be attributed to its different behavior in relation to tooth structure⁽⁵⁾. This failure can be classified into (favorable fracture) that can be repaired and (catastrophic fracture) that forces tooth pulling out and consequential prosthetic interference⁽⁷⁾.

After the successive improvement in the adhesion protocols, bonded restoration can minimize the need

for conventional retention means such as height and taper of the preparation so it can be indicated in cases with no or minimal retention being less traumatic for weakened teeth⁽⁸⁾. An alternative treatment option, endo-crowns, firstly described by Pissis⁽⁹⁾ is bonded overlay restoration consisting of a coronal portion with apical extension that projected into the pulp chamber gaining its macro-mechanical retention from axial walls whereas adhesive resin cement is responsible for its micro-mechanical retention, so this restoration combines the core and crown as a mono-block unit.

Endo-crowns offer a conservative approach especially in teeth with extensive destruction that does not allow adequate ferrule preparation and in limited inter-occlusal space⁽¹⁰⁾. Moreover, fewer clinical steps make it more practical about cost and time-saving than post, core, and crown coordination⁽¹¹⁾. However, RCT molars rebuilt with endo-crowns have been advised with clinical success, but it is quite different in RCT premolars restored with endo-crowns⁽¹²⁾. This is supported by several studies that reported better fracture resistance of ceramic endo-crowns in restoring molars and maxillary premolars than ceramic crowns retained by conventional post-core⁽⁶⁾. However, more frequent challenges are encountered with mandibular premolars due to their coronal and radicular geometries unlike their maxillary counterparts⁽¹³⁾.

CAD-CAM technologies allow the use of a wide collection of available restorative materials through subtractive or additive manufacturing to obtain chair-side fabrication and cementation of final restoration at the same visit of preparation with improved esthetics⁽¹⁴⁾. The success of subtractive manufacturing in dentistry has resulted in a prosthesis with fewer porosities and a more homogenous consistency from solid materials (blocks and discs). After several years of innovation, additive manufacturing through 3D printing technology was introduced as an alternative method

to create a 3D object ⁽¹⁵⁾ through the fusion of liquid or powder materials together layer by layer. It surpasses subtractive manufacturing due to less material waste, its ability to produce larger objects fine details ^(15,16).

This new technology includes digital light processing (DLP), stereolithography (SLA), fused deposition modeling (FDM), material jetting (MJ), and selective laser doping (SLS) ⁽¹⁶⁾. SLA and DLP are more commonly used in-office 3D printers to produce prostheses through photo-polymerization of a monomeric resin ⁽¹⁷⁾. DLP printers utilize a light projector to polymerize a full resin layer in the XY-axis simultaneously resulting in rapid processing with high resolution and low cost ⁽¹⁶⁾, while in SLA one, a laser beam moves across the resin tank to solidify the material layer by layer on the horizontal axis. This point-by-point resin polymerization provides no loss of surface quality making it ideal for millimeter-scale printing ⁽¹⁷⁾. While the DLP technology has potential in dentistry, the resulting surface texture of the outcome object is not regular as in SLA due to the pixel projection ⁽¹⁶⁾.

The selection of suitable CAD-CAM restorative materials with low elastic modulus compatible with those of natural teeth for the fabrication of endo-crowns for premolar teeth assumes to give a biomechanical advantage in endo-crown performance ⁽¹⁸⁾. VarseoSmile Crown plus (VS) becomes now available for additive manufacturing through 3D printing technology which is a newly developed tooth-colored, ceramic-filled hybrid resin material, light-cured plastic based on methacrylic acid esters with a modulus of elasticity 4.09 GPa ⁽¹⁹⁾. On the other side, several materials are available for subtractive manufacturing, Brilliant Crios (BC) (Coltène, Whaledent A.G, Switzerland) which is composite resin reinforced with silica and glass ceramic fillers in a methacrylate matrix that is cross-linked to have a modulus of elasticity 10.3 GPa ⁽²⁰⁾. Also, Bio-HPP which is a modified PEEK reinforced

by 20% ceramic fillers (0.3-0.5 μm grain size) evenly dispersed within the partially crystallized polymer matrix ⁽²¹⁾ having shock-absorbing effect due to reduced modulus of elasticity (3-4 GPa), thus less stresses transmitted to the root and the restoration consequently ⁽²²⁾.

In addition, marginal adaptability is a critical factor affecting the prognosis of any restoration as cement dissolution, microleakage, increased plaque accumulation with subsequent secondary caries, periodontal inflammation, and endodontic failure are sequela of poor margin adaptation ⁽¹⁴⁾, so the long-term survival of dental restorations may strongly be influenced by the complexity of the oral environment with many challenging variables such as acidic or basic pH, humidity, thermal fluctuation, and cyclic loading ⁽²³⁾.

Yet no studies reported the impact of thermo-mechanical aging on the marginal adaptability, fracture resistance, and failure mode of RCT mandibular premolars restored with 3D printed CAD-CAM endo-crowns. Therefore, this study was conducted to assess the marginal adaptability of RCT premolars restored with 3D printed and milled endo-crowns before and after thermo-mechanical aging, fracture resistance, and failure modes. The tested null hypotheses of this study were that no difference would be found (1) in the marginal adaptability of tested 3D printed and milled CAD-CAM endo-crowns before and after thermo-mechanical aging. (2) in the fracture resistance of RCT mandibular premolars restored with tested 3D printed and milled CAD-CAM endo-crowns.

MATERIALS AND METHODS

The minimally accepted sample size calculated was 12 per group According to a previous study ⁽¹⁰⁾, when the response within each subject group was normally distributed with a standard deviation of 454.6, the estimated mean difference was 550, when the power was 80 % & type I error probability was

TABLE (1) Materials' composition and their manufacturers.

Trade name	Composition	Filler Mass (weight %)	Modulus of elasticity	Manufacturer
Varseo Smile Crown plus (VS)	- Silanized dental glass, methyl benzoyl formate, diphenyl (2,4,6-trimethyl benzoyl) phosphine oxide. - 40-isopropylidiphenol, ethoxylated and 2-methylprop-2enoic acid.	0.7 µm particle size forming 30–50 wt. % inorganic filler	4.09 GPa	Bego, Bremen, Germany
Brilliant Crios (BC) blocks size 14 (A3 LT)	- 70.7% <20 nm Amorphous silica and <1 µm barium glass. - 29.3% Cross-linked methacrylate resin matrix (Bis-GMA, Bis-EMA, TEGDMA)	(SiO ₂ < 20 nm, barium glass <1 µm forming 70.7 wt.% inorganic filler	10.3 GPa	Coltène, Whaledent A.G. Altstätten, Switzerland
breCAM.Bio-HPP blank (PEEK)	- Polyether-ether-ketone (PEEK) polymer	0.3 - 0.5 µm ceramic filler grain size Forming 20 wt.%	3-4 GPa	Bredent GmbH & Co KG

Bis-EMA, ethoxylated bisphenol A-glycol dimethacrylate, Bis-GMA, bisphenol A-glycidyl methacrylate, UDMA urethane dimethacrylate, TEGDMA, triethylene glycol dimethacrylate; SiO₂, silicon dioxide.

0.05. P.S 3.1.6 Power software was used to calculate the sample size. A detailed description of the tested materials' composition is listed in Table 1.

Teeth specimen preparation:

Thirty-six mandibular first premolars were collected after extraction for the orthodontic purposes having intact crowns without abrasion cavities and/or caries. (All procedures were performed following the rules of the Research Ethics Committee (FDBSU-REC) of the Faculty of Dentistry, Beni-Suef University, Egypt (Approval number: # # REC-FDBSU/01122022-01/AA).

The collected teeth were immersed in sodium hypochlorite (5%) for 15 min at room temperature for disinfection then scaled under copious water for removal of any organic debris, and finally kept in 0.9% saline (ADWIC, Pharmaceutical division, Abu Zabal, Egypt) until testing procedures. In order to standardize the acrylic blocks, a machine-milled split brass mold was used to vertically mount the tooth specimen in self-curing poly-methyl-methacrylate (PMMA) resin (Acrostone, Egypt) on its longitudinal axis. Teeth specimens were

centralized in the mold where Cemento-Enamel Junction (C.E.J) was 2 mm above resin level using a paralleling device (BEGO, Germany) until resin blocks polymerize completely then kept again in 0.9% saline.

Specimen grouping:

The collected teeth were divided based on the CAD-CAM restorative material type utilized for the construction of endo-crowns into three groups: **3D printed (VS) group:** was assigned for 3D printed endo-crowns fabricated from VarseoSmile Crown plus through the 3D printing technology. **Brilliant Crios (BC) group:** was assigned for milling of endo-crowns from Brilliant Crios blocks. **breCAM. Bio-HPP (PEEK) group:** was assigned for milling of endo-crowns from breCAM.Bio-HPP blank.

Endodontic treatment:

The collected teeth were endodontically prepared using a rotary-files (M-Pro IMD, Guangdong, China) to estimated working length with copious irrigation 5% sodium hypochlorite after each file then obturated with suitable gutta-percha cones (Dentsply Maillefer, Switzerland) and eugenol-free

resin-based sealer (Adseal, Metabiomed, Korea) to prevent intervention with polymerization of resin cement. Finally, a hot instrument was used to cut excess gutta-percha.

Endo-crown preparation:

Decoronation of teeth was performed 2 mm coronal to C.E.J. perpendicular to their longitudinal axis producing a flat surface utilizing an electrical saw (Isomet 4000, micro saw, Buehler Ltd, USA) with rotating speed 2500 rpm and water coolant feeding rate 5 mm/min utilizing diamond disc (Buehler instrument, USA) having 0.6 mm thickness.

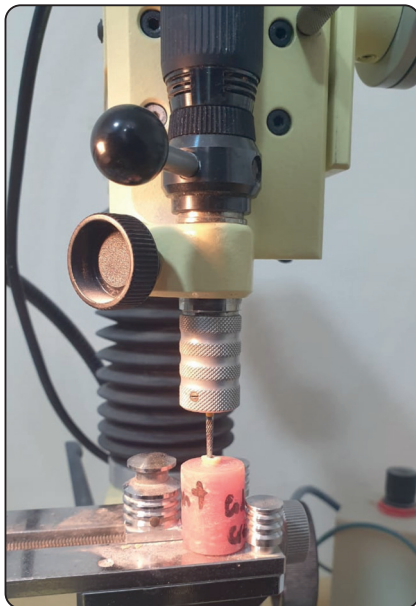


Fig. (1) Endo-crown preparation.

An even cavity preparation was done by the same operator using a dental milling surveyor (Bredent BF2, Bredent GmbH & Co.KG, Germany) in all teeth with butt joint design. The preparation of the pulp chamber was performed to remove undercuts and obtain internal taper of axial walls with 8-10 degrees using a tapered stone with a flat end (Mani Dia-burs TR-12, Japan). A digital caliper was used to ensure the axial wall thickness having 2 mm with an accuracy of ± 0.01 mm. The preparations

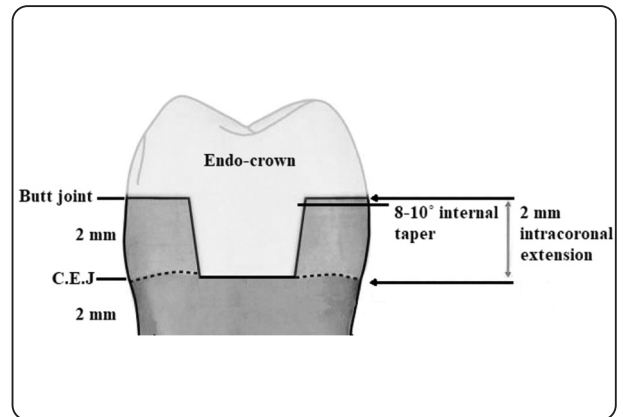


Fig. (2): Schematic diagram showing endo-crown preparation design.

were finished using a round polishing bur (Bredent GmbH & Co.KG, Germany) to have a central cavity of 2 mm depth from the occlusal surface which was checked using a periodontal probe ⁽²⁴⁾.

Endo-crown Fabrication

Using an extra-oral scanner (AutoScan DS-EX, Shining 3D, Hangzhou, China), the prepared teeth were scanned, and an endo-crown was designed on the obtained virtual model using a software program (exocad Dental DB 3.0 Galway, exocad GmbH, USA), Figure (3, 4). The design parameters such as the spacer thickness were set to be 10 μ m. All endo-crowns were designed to have the same occlusal anatomy and occluso-gingival length with an axial thickness of 1.5 mm ⁽²⁵⁾.

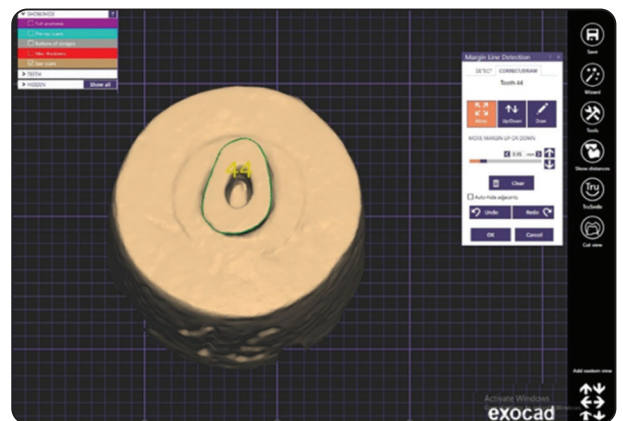


Fig. (3) Optical scan and margin line detection for a representative preparation for endo-crown fabrication.

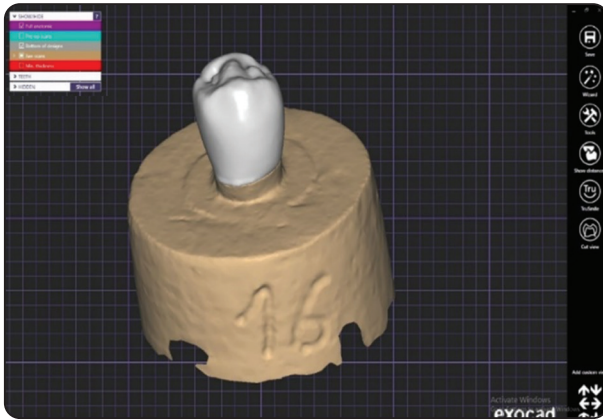


Fig. (4): Restoration proposal for endo-crown.

For the 3D printed (VS) group, the finished STL file was printed using DLP technology utilizing a 3D printer (Anycubic photon S, Shenzhen, China) from a liquid material VarseoSmile Crown plus (VS) where 3D printing software (Chitobox V1.9.0, Shenzhen, China) was used to prepare resin optimized for VS having 0.05 mm layer height, bottom layer count 8, 6.5 seconds exposure time, 20 seconds bottom exposure, 5 mm lift distance and 60mm/sec lift speed. On completion of printing, the 3D printed endo-crowns were separated from the build platform and cleaned following manufacturing recommendation with ethanol (96%) using an unheated ultrasonic bath (Anycubic 3D Printer Wash and Cure Machine 2.0). Firstly, the cleaning process was performed for 3 min in a reusable ethanol solution (96 %) and then for another 2 min in a freshly used ethanol (96 %) solution.

Finally, the 3D printed endo-crowns were eliminated from the ethanol bath and then sprayed with additional ethanol (96 %) to totally get rid of any remnant resin residue followed by air drying using compressed air under an extraction unit. Post-curing of the printed endo-crowns was performed two times for 45 min each in an ultraviolet light curing device (Anycubic 3D Printer Wash and Cure Machine 2.0) appropriate for post-curing of 3D printed composite resin materials to guarantee full polymer conversion reducing residual monomer

thus obtaining the highest mechanical properties. After cooling time (3-5 min), all supporting structures of the final printed end-product were cut with a cutting wheel.

For the milled groups, the finished STL file was exported to a 5-axis CAD-CAM milling machine (SHERA Eco-mill 5X, Germany) to cut monolithic endo-crowns of Brilliant Crios blocks size 14 (A3 LT, 14 × 12 × 18 mm) for Brilliant Crios (BC) group and of breCAM.Bio-HPP blank for PEEK group. The milling process was performed under a copious amount of water irrigation. All milled endo-crowns were fitted on corresponding teeth to check the marginal adaptability using an explorer. Finishing of endo-crowns of VS and BC groups was performed using a composite polishing kit (AZDENT RA0309, Mainland, China) according to a previous study⁽²⁶⁾ to get perfectly smooth surface, while for the PEEK group, a goat-hair brush with Acrypol pre-polishing paste was used to obtain smooth surface according to the recommendations of the manufacturer.

Bonding procedures

The internal surface of each endo-crown was prepared by sandblasting in a sandblaster (Basic Classic blaster, 70-250 μm , 220-240 V Renfert GmbH, Germany) following the manufacturer's recommendation for the respective restorative material. For the VS group, 110 μm Al_2O_3 at a pressure of 1.5 bar, for the BC group, 25-50 μm Al_2O_3 at a pressure of 1.5 bar, and for the PEEK group, 110 μm Al_2O_3 at 2.5 bar. The endo-crowns were then thoroughly cleaned in an ultrasonic cleaner (CD-4820, CODYSON, Guangdong, China) for 10 minutes with distilled water followed by air drying. The internal surface of each endo-crown was coated with a dental adhesive (One coat 7 universal, Coltene, Switzerland) using a disposable brush and rubbed for 20 seconds for VS and BC group while bonding agent (visio.link, Bredent GmbH & Co.KG, Germany) was applied then cured in light curing unit (Brelux Power Unit; bredent) at 220 mW/cm^2 for 1.5 minutes for PEEK group.

After air drying the dentin surface of each tooth by oil-free air, a disposable brush was used to apply dental adhesive (One coat 7 universal, Coltene, Switzerland) and rubbed for 20 seconds, then gently air dried for 5 seconds then light cured for 10 seconds. A self-adhesive resin cement (SoloCem, Coltene, Switzerland) was used to bond endo-crowns of all tested groups to the dentin surface. Each endo-crown was seated in place by light pressure then the excess cement was removed after 3 seconds of initial polymerization then the chemical setting of cement was completed under a load of 5 kilograms followed by light curing for 40 seconds using a light-curing unit (Woodpecker LED-D Wireless, Mident Industrial Co., China). Lastly, all specimens were kept in distilled water at room temperature till the testing procedure.

Thermo-mechanical aging

Mechanical aging of the specimens was done using a chewing simulator (Robota, ACH-09075DC-T, AD Tech Technology Co. Ltd, Germany). The teeth with cemented endo-crowns were fixed in the Teflon housing of the sample holder and subjected to 60000 loading cycles at a frequency of 1.6 Hz under a weight of 10 kg (98 N) utilizing a metallic rod with a 3.8 mm diameter round tip parallel to the long axis while immersed under distilled water at 37°C⁽²³⁾.

After completion of the mechanical aging procedures, all specimens were exposed to 5000 thermocycles (between 55°C and 5°C)⁽²⁷⁾ in an automated thermocycling machine (Robota automated thermal cycle; BILGE, Turkey) with dwell times of 25 seconds in each water bath and a lag time of 10 seconds.

Marginal gap measurements

A digital microscope (U500x Digital Microscope, Guangdong, China) was utilized to measure the marginal gap before and after thermo-mechanical aging. The images were taken at a constant magnification of 40X for the marginal gap

measurement by digital image analysis software (Image J 1.43U, National Institute of Health, USA). For each specimen, the measurements were performed for each shot at four equidistant landmarks along the contour for each surface (mesial, distal, buccal, lingual). The measurement at each point was recorded three times then data collection, tabulation, and statistical analysis were performed.

Fracture resistance test

After marginal gap assessment, All specimens were then loaded vertically using a universal testing machine (Model 3345; Instron Industrial Products, Norwood, MA, USA) with a loadcell of 5 kN where the specimens were tightened to the lower fixed compartment and a compressive load was applied at a cross-head speed of 1mm/min to the center of the occlusal table of endo-crown using a metallic rod with 3.8 mm diameter round tip mounted to the upper movable compartment of the testing machine. A computer software (Instron® Bluehill Lite Software) recorded the data where the load at failure was evidenced by an audible crack and assured by a sudden fall at the stress-strain curve. The fracture load was recorded in Newton and failure mode was evaluated for each specimen and categorized as follows:

- I. Repairable (favorable) fractures:** include complete or partial de-bonding of the endo-crown without fracture, fracture of the endo-crown without fracture of tooth, or fracture of the endo-crown/tooth complex above bone level simulation.
- II. Catastrophic (non-repairable) fractures:** include fracture of the endo-crown/tooth complex below bone level simulation.

Statistical analysis

The data were statistically analyzed with statistical software (SPSS 16, IBM, Armonk, NY). Exploration of the obtained data was done

using Shapiro-Wilk test and Kolmogorov-Smirnov test for normality which showed that all groups regarding marginal gap (μm) and fracture resistance (N) originated from normal distribution (parametric data) resembling normal Bell curve. Consequently, comparison between groups was performed using One Way ANOVA test followed by Tukey's Post Hoc test, while comparison between different intervals was performed by using Paired t-test.

RESULTS

The specimens of all tested groups survived the thermo-mechanical aging without any signs of detectable failure.

Marginal gap measurements

Effect of thermo-mechanical aging

The mean, standard deviations (SD) values and statistical results of the marginal gap were recorded in μm before and after thermo-mechanical aging at selected points on all surfaces, and the overall marginal gap values, for all tested groups were listed in Table 2. Paired t-test revealed a significant increase in the overall marginal gap values after thermo-mechanical aging of all tested groups: 3D printed (VS) group ($P=0.04$), Brilliant Crios (BC) group ($P=0.02$), and breCAM.Bio-HPP (PEEK) group ($P=0.0003$).

TABLE (2) Marginal gap values (μm) before and after thermo-mechanical aging at selected points on all surfaces of all tested groups and comparison between them:

Effect of treatment		Marginal gap								
		Before		After		Difference				
		M	SD	M	SD	MD	SEM	95% CI		P value
								L	U	
3D printed (VS) group	Buccal	41.42	12.53	55.35	16.6	13.93	6.21	0.25	27.5	0.04*
	Lingual	50.77	14.33	56.81	14.69	6.03	7	-9.37	21.45	0.41
	Mesial	54.97	17.75	63.37	10.26	8.39	4.26	-0.98	17.78	0.07
	Distal	45.86	13.75	62.21	17.18	16.36	6.35	2.35	30.35	0.02*
	Overall	48.26	10.78	59.44	8.08	11.18	3.08	4.38	17.97	0.04*
Brilliant Crios (BC) group	Buccal	51.9	20.63	62.42	19.91	10.52	5.61	-2.6	23.65	0.15
	Lingual	48.94	10.65	56.34	27.16	7.40	7.73	-9.61	24.4	0.35
	Mesial	51	17.07	66.71	18.57	15.71	8.91	-3.91	35.32	0.105
	Distal	60.64	22.38	76.23	20.41	15.59	8.42	-2.94	34.12	0.09
	Overall	53.12	11.81	65.42	12.39	12.31	4.85	1.61	23	0.02*
PEEK group	Buccal	38.13	11.87	47.38	12.46	9.24	5.18	-2.16	20.66	0.11
	Lingual	35.12	8.53	51.71	10.88	16.59	3.57	8.73	24.45	0.0007*
	Mesial	45.43	15.73	53.19	17.01	7.76	5.04	-3.34	18.87	0.16
	Distal	41.72	14.91	53.69	9.21	11.97	4.56	1.92	22.01	0.02*
	Overall	40.1	6.46	51.49	8.41	11.39	2.16	6.63	16.15	0.0003*

M: mean *SD: standard deviation*

MD: mean difference

CI: confidence interval

**significant difference as $P < 0.05$.*

SEM: Standard error mean

L: lower arm

U: upper arm

Effect of material

The mean, standard deviations (SD) values, and statistical results of the marginal gap were recorded in μm of all tested groups at selected points on all surfaces and the overall marginal gap values, before and after thermo-mechanical aging and difference between them were listed in Table 3 and Figure 5. One Way ANOVA test showed a significant difference between the marginal gap values of all tested groups. Tukey's Post Hoc test revealed a significant difference between the overall marginal gap values of all tested groups before and after thermo-mechanical aging where breCAM. Bio-HPP (PEEK) group recorded significantly the lowest value (before 40.10 ± 6.46 , after 51.49 ± 8.41), Brilliant Crios (BC) group recorded

significantly the highest value (before 53.12 ± 11.81 , after 65.42 ± 12.39), while 3D printed (VS) group revealed insignificant difference with other groups (before 48.26 ± 10.78 , after 59.44 ± 8.08). Regarding the difference in the overall marginal gap values (after-before), there was an insignificant difference between all tested groups.

Fracture resistance test

The mean, standard deviation (SD) values, and statistical results of the fracture resistance recorded in Newton of all tested groups were listed in Table 4 and Figure 6. One Way ANOVA test revealed a significant difference between fracture resistance mean values of all tested groups ($P < 0.0001$). Tukey's Post

TABLE (3) Marginal gap values (μm) at selected points on all surfaces of all tested groups and comparison between them:

Effect of material		Marginal gap						P value
		3D printed (VS) group		Brilliant Crios (BC) group		PEEK group		
		M	SD	M	SD	M	SD	
Before	Buccal	41.42 ^a	12.53	51.90 ^a	20.63	38.13 ^a	11.87	0.09
	Lingual	50.77 ^a	14.33	48.94 ^a	10.65	35.12 ^b	8.53	0.003*
	Mesial	54.97 ^a	17.75	51.00 ^a	17.07	45.43 ^a	15.73	0.93
	Distal	45.86 ^{ab}	13.75	60.64 ^a	22.38	41.72 ^b	14.91	0.03*
	Overall	48.26 ^{ab}	10.78	53.12 ^a	11.81	40.10 ^b	6.46	0.01*
After	Buccal	55.35 ^a	16.6	62.42 ^a	19.91	47.38 ^a	12.46	0.11
	Lingual	56.81 ^a	14.69	56.34 ^a	27.16	51.71 ^a	10.88	0.76
	Mesial	63.37 ^a	10.26	66.71 ^a	18.57	53.19 ^a	17.01	0.11
	Distal	62.21 ^{ab}	17.18	76.23 ^a	20.41	53.69 ^b	9.21	0.006*
	Overall	59.44 ^{ab}	8.08	65.42 ^a	12.39	51.49 ^b	8.41	0.005*
Difference	Buccal	13.93 ^a	21.51	10.52 ^a	20.66	9.25 ^a	17.95	0.84
	Lingual	6.04 ^a	24.26	7.40 ^a	26.79	16.59 ^a	12.37	0.81
	Mesial	8.40 ^a	14.77	15.71 ^a	30.87	7.76 ^a	17.48	0.62
	Distal	16.36 ^a	22.02	15.59 ^a	29.17	11.97 ^a	15.81	0.88
	Overall	11.18 ^a	10.69	12.31 ^a	16.83	11.39 ^a	7.49	0.97

M: mean SD: standard deviation *significant difference as $P < 0.05$.
 same superscript letters within same row were insignificantly different as $P > 0.05$.
 different superscript letters within same row were significantly different as $P < 0.05$.

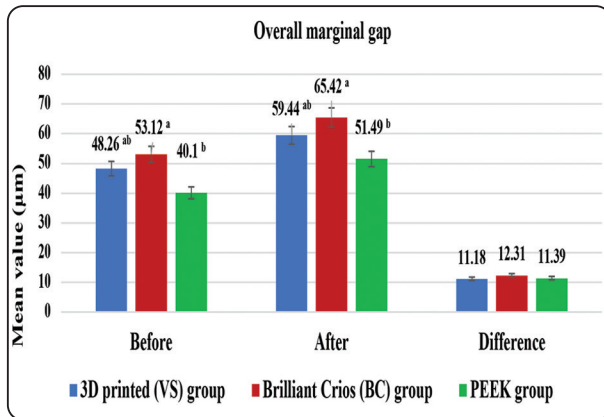


Fig. (5): Bar chart representing marginal gap before, after thermo-mechanical aging and difference between them in all tested groups.

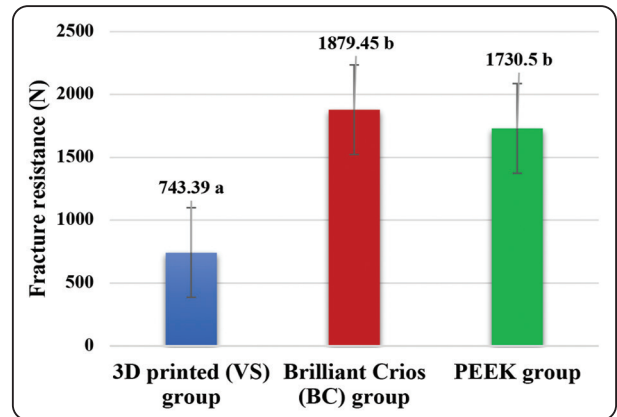


Fig. (6): Bar chart representing mean and standard deviation values of fracture resistance (N) in all tested groups.

Hoc test showed an insignificant difference between Brilliant Crios (BC) group (1879.45 ± 477.60) and PEEK group (1730.5 ± 210.56); both were statistically significantly higher than that of the 3D printed (VS) group (743.39 ± 68.71).

Failure mode analysis

The repairable (favorable) type was the dominant mode of failure after the evaluation of all failed specimens.

TABLE (4) The mean and standard deviation (SD) load values of the fracture resistance (N) of all tested groups and comparison between them:

Fracture resistance	M	SD	P value
3D Printed (VS) group	743.39 ^a	68.71	
Brilliant Crios (BC) group	1879.45 ^b	477.60	<0.0001*
PEEK group	1730.50 ^b	210.56	

*M: mean SD: standard deviation *significant difference as P < 0.05. same superscript letters within same column were insignificantly different as P > 0.05. different superscript letters were significantly different as P < 0.05.*

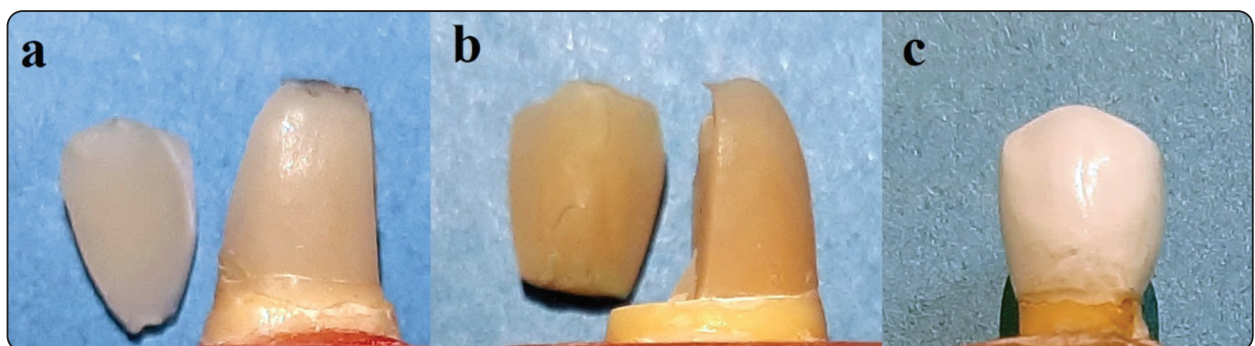


Fig. (7): Mode of failure in endo-crowns of tested groups: a. 3D printed (VS), b. Brilliant Crios, c. PEEK group.

DISCUSSION

Endo-crown restorations have been developed as an alternative treatment for endodontically treated teeth in conjunction with adhesive dentistry. This minimally invasive concept preserves maximum tooth structure for bonding in addition to the utilization of pulp chamber space for improvement of the stability and retention of the restoration. Also, it offers an advantage in case of short clinical crowns, curved roots, and calcified canals that not permitting post applications^(10,11,28).

Together with acceptable esthetics, less clinical time, and reduced bonding interfaces consequently rendering the restoration less prone to adverse marginal degradation of the hybrid layer. Also, the elimination of drilling procedures minimizes the possibility of root fracture risk⁽²⁸⁾.

Despite the increased variability of using natural teeth, it is more closely simulated clinical situations regarding tooth morphology, pulp chamber contour, and the crown/root ratio⁽²⁹⁾. Mandibular premolars were chosen in the present study due to their special anatomy and unique morphology with subsequent cusp deflection and fracture under occlusal forces^(5,6). Additionally, butt joint margin design was applied to exclude any effect of the margin type and their curvature on the marginal adaptability of the restoration⁽³⁰⁾. The preparation was performed to allow for 2 mm intra-coronal extension according to a previous study⁽²⁴⁾ that assessed the endo-crown extension depth on the fracture resistance of mandibular molar and stated that intra-coronal extension of 2 mm revealed higher fracture resistance and accompanied with less non-restorable root fractures than that restored with deep pulpal extensions.

The application of CAD-CAM technology with restorative materials having low elastic modulus for endo-crowns fabrication may theoretically improve the mechanical behavior of the tooth-restoration system due to their bending tendency

under loading and better stress distribution and consequently reducing catastrophic fractures⁽¹⁸⁾. These materials offer greater resiliency and less abrasion to the antagonists than dental ceramics, despite their lower resistance to wear⁽³¹⁾. Moreover, manufacturers pretend better machinability of these materials due to less susceptibility for fracture and chipping attributed to their Young moduli. Additionally, easier repairing and polishing than glass ceramics⁽³²⁾. Despite the clinical privileges of a restorative material with resiliency that might appear obvious, it would suffer from repeated elastic deformation at margins that might trigger microleakage and subsequent restorative failure paired with recurrent decay⁽³¹⁾.

The tested materials were: VarseoSmile Crown Plus (VS), Brilliant Crios (BC), and breCAM.Bio-HPP (PEEK) with a modulus of elasticity 4.09⁽¹⁹⁾, 10.3⁽²⁰⁾, 3-4^(21,22) GPa successively which are comparable with that of dentin (5.5-19.3 GPa)⁽⁵⁾.

Optimal marginal adaptability ensures minimal cement thickness preventing microleakage that could result in failure of the restoration. Also, a thick cement layer will result in interfacial stresses due to increased polymerization shrinkage which may reduce the fracture resistance of the restorations^(14,33).

The measurement of the space between the margin of the restoration and the finish line which is defined as the marginal gap was selected to assess the marginal adaptability⁽³³⁾. Several methods have been reviewed for the measurement of marginal gap including the direct-view method which was the most utilized (47.5%), followed by the cross-sectioning method (23.5%), and the impression replica method (20.2%)⁽³⁴⁾.

In the present study, marginal adaptability was assessed by measurement of the marginal gap through direct viewing with a digital microscope, which is non-invasive, precise, cheap, less time-consuming, less error accumulated from multiple steps, and reproducible method⁽³⁴⁾ but it has some

limitations such as difficult selection of the points at which the measurement of the margin is to be performed, incapacity to distinguish between the tooth and shaded cement or recognizing the most apical part of the finish line. In addition, margins may appear rounded for both die and crown under magnification.

In the present study, 12 specimens per tested group and 16 measurement locations per crown were selected for evaluation of the marginal adaptability of endodontically treated premolars restored with 3D printed and milled endo-crowns before and after thermo-mechanical aging. There was a statistically significant increase in the overall marginal gap values after thermo-mechanical aging of all tested groups: 3D printed (VS) group ($P = 0.04$), Brilliant Crios (BC) group ($P = 0.02$) and breCAM Bio-HPP (PEEK) group ($P = 0.0003$) thus, the first null hypothesis tested in the present study stated that no difference would be found before and after thermo-mechanical aging in the marginal adaptability of tested 3D printed and milled CAD-CAM endo-crowns was rejected. The obtained results revealed that overall marginal gap mean values of the 3D printed (VS) group had an insignificant difference with Brilliant Crios (BC) and breCAM Bio-HPP (PEEK) groups before and after thermo-mechanical aging.

To the authors' knowledge, limited data is available about 3D printed (VS) endo-crowns regarding the marginal gap and fracture resistance. However, a previous study by Donmez et al⁽³⁵⁾ revealed that 3D printed composite resin crowns provided the lowest marginal gap values than other milled resin-based composite crowns. Also, a study by Alharbi et al⁽³⁶⁾ reported that the 3D printed crowns revealed significantly lower marginal gaps than milled ones. Another study by Kakinuma et al⁽³⁷⁾ evaluated the dimensional accuracy of 3D printed and milled resin composite crowns. They concluded that 3D printed crowns revealed fewer

marginal discrepancies with higher accuracy than milled crowns regardless of the abutment form.

Although limited data in the literature about the marginal fit of PEEK as an endo-crown has been reported, the overall marginal gap mean value recorded in the present study before thermo-mechanical aging was ($40.10 \pm 6.46 \mu\text{m}$) which is lower than recorded in a previous study ($81.28 \pm 10.92 \mu\text{m}$)⁽³⁸⁾. The recorded overall marginal gap mean value of Brilliant Crios (BC) group (53.12 ± 11.81) was slightly higher than that recorded by a previous study which was (50.58 ± 4.81)⁽³⁹⁾.

Although the marginal adaptability of CAD-CAM restorations is regarded as material dependent⁽¹⁴⁾, it can be improved with luting cement that is susceptible to dissolution⁽⁴⁰⁾. So, the vertical marginal gap is considered the most crucial in the margin assessment of the crown. No consensus has been reported about the ideal marginal gap, but the maximum clinically accepted marginal gap has been stated to be $120 \mu\text{m}$ ^(35,41).

For better assessment under clinically simulated conditions, artificial aging was performed by subjecting the tested groups to dynamic loading combined with thermocycling⁽³³⁾. To simulate the clinical situation of complex oral environment, all tested groups were subjected to thermo-mechanical aging by application of 60000 loading cycles equivalent to 6 months of clinical service⁽²³⁾ and 5000 thermo-cycles which correspond to 6 months⁽²⁷⁾ of physiological aging in the oral cavity.

Regarding the marginal gap, One Way ANOVA test showed a significant difference between the marginal gap values of all tested groups. Tukey's Post Hoc test revealed a significant difference between the overall marginal gap values of all tested groups before and after thermo-mechanical aging where PEEK group recorded significantly the lowest value (before 40.10 ± 6.46 , after 51.49 ± 8.41), Brilliant Crios (BC) group recorded significantly the highest value (before 53.12 ± 11.81 , after 65.42 ± 12.39),

while 3D printed (VS) group revealed insignificant difference with other groups (before 48.26 ± 10.78 , after 59.44 ± 8.08). Regarding the difference in the overall marginal gap values (after-before thermo-mechanical aging), there was an insignificant difference between all tested groups.

In the present study, thermo-mechanical aging led to a statistically significant increase in the marginal gap mean values. This can be attributed to the accelerated hydrolysis of unprotected collagen fibers and extraction of poorly polymerized resin tags due to exposure to hot water. In addition to generated stresses at the tooth/restoration interface due to a mismatch in the coefficient of thermal expansion of tooth structure and restorative material which have been suggested as a crucial factor for deterioration of the marginal adaptability⁽⁴²⁾. These alterations in temperatures can cause expansion and contraction of the restorative materials resulting in stresses, crack formation, and propagation due to a mismatch in the coefficient of thermal expansion of the resin matrix and the filler particles⁽⁴³⁾.

The results of the present study were in accordance with Krejci et al⁽⁴⁴⁾ who found a significant negative effect of thermo-mechanical aging on the marginal fit of the crowns, but this is against the findings of Beschmidt and Strub⁽⁴⁵⁾ who reported that the aging procedure had no significant effect on the marginal fit.

Although the overall marginal gap mean values of all tested groups were increased after thermo-cycling aging but still below the clinically accepted limit of $120 \mu\text{m}$ ^(35,41). All tested groups survived the thermo-mechanical aging which may be attributed to the good mechanical reliability of the endo-crown restoration and durable adhesion obtained from adequate tooth structure, proper restoration preparation according to manufacturer recommendation, and the usage of MDP-based resin cement⁽⁴⁶⁾.

In the present study, no periodontal ligament simulation was performed as it may alter fracture resistance and fracture mode⁽⁴⁷⁾. The specimens

were loaded vertically by application of compressive load along the long-axis teeth. The obtained results revealed a significant difference between fracture resistance mean values of all tested groups ($P < 0.0001$) so the second null hypothesis tested in the present study stated that no difference would be found in the fracture resistance of RCT mandibular premolar restored with tested 3D printed and milled CAD-CAM endo-crowns was rejected. There was an insignificant difference between fracture resistance mean values of Brilliant Crios (BC) (1879.45 ± 477.60 N) and breCAM Bio-HPP (PEEK) groups (1730.5 ± 210.56 N); both were statistically significantly higher than that of 3D printed (VS) group (743.39 ± 68.71 N).

This finding could be attributed to the variations in the microstructure, chemical composition, and mechanical properties of tested CAD-CAM restorative endo-crowns which had different flexural strength, fracture toughness, and different filler content. The milling of endo-crowns from blocks and discs that were industrially fabricated under high pressure and high temperature leads to a higher volume fraction of filler and higher rates of conversion such as Brilliant Crios (BC) which is reinforced composite resin with amorphous silica and glass ceramic fillers (about 70.7 wt.%) in methacrylate matrix that is cross-linked to have a modulus of elasticity 10.3 GPa and flexural strength (198 MPa) and fracture toughness ($1.5 \text{ MPa}\cdot\text{m}^{1/2}$)⁽²⁰⁾. Also, breCAM Bio-HPP (PEEK) CAD-CAM blanks fabricated industrial pre-pressing process under optimal conditions show a reduced porosity and therefore improve their mechanical properties such as flexural strength (140-170 MPa), fracture toughness ($2.7\text{-}4.3 \text{ MPa}\cdot\text{m}^{1/2}$) beside similar elastic properties (3-4 GPa)^(5,21,22) which is comparable with that of dentin (5.5-19.3 GPa)⁽⁵⁾. This shock-absorbing effect reduces the stresses transmitted to the restoration and the root accordingly⁽²²⁾. In addition to ceramic fillers (about 20 wt.%) with 0.3-0.5 μm grain size that are equally distributed in the polymer matrix that is

partially crystallized⁽²¹⁾. While in the 3D printed (VS) group, the lower fracture resistance may be attributed to the high probability of residual monomers in 3D printed restoration in comparison to milled resins which might have a quite possible influence on bonding⁽⁴⁸⁾.

The recorded fracture resistance values in the present study are comparable with that of a previous study⁽¹⁰⁾ evaluated the fracture strength of endo-crowns restored with different hybrid blocks and lithium disilicate glass ceramics under axial and lateral forces where Brilliant Crios endo-crowns showed highest fracture strength under axial loading which may be attributed to matching between elastic modulus of Brilliant Crios and dentine leading to a similar degree of plastic deformation in both the restoration and underlying dentine so better load transmission to dentin rather than concentrated within the restoration. Together, the chemical similarity between the reinforced composite block and adhesive resin cement in composition ensures high bonding capacity between them.

Although limited data in the literature about fracture resistance 3D printed endo-crowns, a previous study⁽⁴⁹⁾ found no statistically significant differences between the fracture load of CAD-CAM crowns fabricated from 3D printed or milled. Hence these results cannot be compared with that of the present study due to differences in the whole study setup, abutment design, and its material properties because the used die fabricated with SLA technology has a low elastic modulus of 2.5 GPa compared with that of human dentin.

The fracture resistance mean values recorded in the present study were above the bite force estimated in the premolar region during function (520N)⁽⁵⁰⁾. Regarding the failure mode, all tested groups showed repairable type which is consistent with Acar et al⁽¹⁰⁾ who reported that repairable failure was the most prevalent under different loading with the majority of failure being cohesive. Also, this is in agreement with that of El-Damanhoury et al⁽⁵⁾ who

reported that hybrid CAD-CAM composite endo-crowns did not show catastrophic failure mode. This may be attributed to the concentration of stresses at the adhesive interface causing cohesive failure of the resin cement resulting in the de-bonding of such endo-crowns. Also, the smaller surface area available for bonding together with higher crown the height of premolars may compromise the mechanical properties of the endo-crown/tooth complex.

Thermo-mechanical aging was performed for a limited number of 5000 thermocycles equivalent to only 6 months of clinical surface⁽²⁷⁾ which is considered a limitation of the present study, so more research is needed to simulate long-term oral performance for better evaluation of the durability of endo-crowns restorations. Also, the incorporation of artificial saliva is needed.

CONCLUSIONS

Within the limitations of this study, the following can be withdrawn:

1. Marginal adaptability of the (breCAM.Bio-HPP) PEEK endo-crowns were better than Brilliant Crios and 3D printed (VarseoSmile Crown Plus (VS)) endo-crowns (BC) before and after thermo-mechanical aging.
2. Thermo-mechanical aging had resulted in a significant reduction of the marginal adaptability of all tested endo-crowns, but all recorded marginal gap mean values were within the clinically acceptable range.
3. The fracture resistance of Brilliant Crios endo-crowns was higher than (breCAM.Bio-HPP) PEEK and 3D printed (VarseoSmile Crown Plus (VS)) endo-crowns, but all recorded fracture load values were above the estimated bite force in the premolar region.
4. Regarding the failure mode, all tested endo-crowns showed repairable (favorable) fractures.

REFERENCES

1. Schwartz RS, Robbins JW. Post placement and restoration of endodontically treated teeth: a literature review. *J Endod*. 2004; 30:415-289-301.
2. Veselinovi V, Todorovi A, Lisjak D. Restoring endodontically treated teeth with all-ceramic endo-crowns: case report. *Stomatol Glas Srb*. 2008; 55:54-64.
3. Lanza A, Aversa R, Rengo S, Apicella D, Apicella A. 3D FEA of cemented steel, glass and carbon posts in a maxillary incisors. *Dent Mater*. 2005; 21:709-15.
4. Al-Dabbagh RA. Survival and success of endocrowns: A systematic review and meta-analysis. *J Prosthet Dent*. 2021;125(3):415.e1-415.e9.
5. El-Damanhoury HM, Haj-Ali RN, Platt JA. Fracture resistance and microleakage of endocrowns utilizing three CAD-CAM blocks. *Oper Dent*. 2015;40(2):201-210.
6. Govare N, Contrepolis M. Endocrowns: A systematic review. *J Prosthet Dent*. 2020;123(3):411-418.e9.
7. Dietschi D, Duc O, Krejci I, Sadan A. Biomechanical considerations for the restoration of endodontically treated teeth: a systematic review of the literature, Part II (Evaluation of fatigue behavior, interfaces, and in vivo studies). *Quintessence Int*. 2008;39(2):117-129.
8. Conrad HJ, Seong WJ, Pesun IJ. Current ceramic materials and systems with clinical recommendations: A systematic review. *J Prosthet Dent*. 2007; 98:389-404.
9. Pissis P. Fabrication of a metal-free ceramic restoration utilizing the monobloc technique. *Pract Periodontics Aesthet Dent*. 1995;7(5):83-94.
10. Acar DH, Kalyoncuoglu E. The fracture strength of endocrowns manufactured from different hybrid blocks under axial and lateral forces. *Clin Oral Investig*. 2021;25(4):1889-1897.
11. Pedrollo Lise D, Van Ende A, De Munck J, Umeda Suzuki TY, Cardoso Vieira LC, Van Meerbeek B. Biomechanical behavior of endodontically treated premolars using different preparation designs and CAD/CAM materials. *J Dent*. 2017;59:54-61.
12. Bindl A, Richter B, Mormann WH. Survival of ceramic computer-aided design/manufacturing crowns bonded to preparations with reduced macroretention geometry. *Int J Prosthodont* 2005;18:219-24.
13. Guo J, Wang Z, Li X, Sun C, Gao E, Li H. A comparison of the fracture resistances of endodontically treated mandibular premolars restored with endocrowns and glass fiber post-core retained conventional crowns. *J Adv Prosthodont*. 2016;8(6):489-493.
14. El Ghoul WA, Özcan M, Ounsi H, Tohme H, Salameh Z. Effect of different CAD-CAM materials on the marginal and internal adaptation of endocrown restorations: An in vitro study. *J Prosthet Dent*. 2020;123(1):128-134.
15. Naseer MU, Kallaste A, Asad B, Vaimann T, Rassölkin A. A Review on Additive Manufacturing Possibilities for Electrical Machines. *Energies*. 2021;14(7):1940.
16. Kim GT, Go HB, Yu JH, et al. Cytotoxicity, Colour Stability and Dimensional Accuracy of 3D Printing Resin with Three Different Photoinitiators. *Polymers (Basel)*. 2022;14(5):979.
17. Moon W, Kim S, Lim BS, Park YS, Kim RJ, Chung SH. Dimensional Accuracy Evaluation of Temporary Dental Restorations with Different 3D Printing Systems. *Materials (Basel)*. 2021;14(6):1487.
18. Hassouneh L, Jum'ah AA, Ferrari M, Wood DJ. Post-fatigue fracture resistance of premolar teeth restored with endocrowns: An in vitro investigation. *J Dent*. 2020;100:103426.
19. Scientific Studies on VarseoSmile Crown plus. Available online: https://www.bego.com/fileadmin/user_downloads/Mediathek/3D-Druck/Scientific-Studies/VarseoSmileCrown-plus/EN/de_81022_0000_br_en.pdf (accessed on 19 May 2021).
20. Hampe R, Theelke B, Lümekemann N, Eichberger M, Stawarczyk B. Fracture Toughness Analysis of Ceramic and Resin Composite CAD/CAM Material. *Oper Dent*. 2019;44(4):E190-E201.
21. Najeeb S, Zafar MS, Khurshid Z, Siddiqui F. Applications of polyetheretherketone (PEEK) in oral implantology and prosthodontics. *J Prosthodont Res*. 2016;60(1):12-19.
22. Papathanasiou I, Kamposiora P, Papavasiliou G, Ferrari M. The use of PEEK in digital prosthodontics: A narrative review. *BMC Oral Health*. 2020;20(1):217.
23. Nawafleh N, Hatamleh M, Elshiyab S, Mack F. Lithium Disilicate Restorations Fatigue Testing Parameters: A Systematic Review. *J Prosthodont*. 2016;25(2):116-126.
24. Hayes A, Duvall N, Wajdowicz M, Roberts H. Effect of Endocrown Pulp Chamber Extension Depth on Molar Fracture Resistance. *Oper Dent*. 2017;42(3):327-334.
25. Tartuk BK, Ayna E, Göncü Başaran E. Comparison of the Load-bearing Capacities of Monolithic PEEK, Zirconia and Hybrid Ceramic Molar Crowns. *Meandros Medical and Dental Journal*. 2019;20(1):45-50.
26. Alharbi N, Wismeijer D, Osman RB. Additive Manufacturing Techniques in Prosthodontics: Where Do We Currently Stand? A Critical Review. *Int J Prosthodont*. 2017; 30(5):474-484.

27. Gale MS, Darvell BW. Thermal cycling procedures for laboratory testing of dental restorations. *J Dent.* 1999;27(2):89-99.
28. Halim CH, Taymor M, Sadek HS. Fracture resistance and failure mode of endodontically treated premolars and molars restored with two different treatment modalities: an in vitro study. *Egyptian Dental Journal* 2015;(61): 2801-2815.
29. Chang CY, Kuo JS, Lin YS, Chang YH. Fracture resistance and failure modes of CEREC endo-crowns and conventional post and core-supported CEREC crowns. *J Dent Sci* 2009;4:110-7.
30. Burke FJ. Tooth fracture in vivo and in vitro. *J Dent.* 1992;20(3):131-139.
31. Awada A, Nathanson D. Mechanical properties of resin-ceramic CAD/CAM restorative materials. *J Prosthet Dent.* 2015;114(4):587-593.
32. Ruse ND, Sadoun MJ. Resin-composite blocks for dental CAD/CAM applications. *J Dent Res.* 2014;93(12):1232-1234.
33. Taha D, Spintzyk S, Sabet A, Wahsh M, Salah T. Assessment of marginal adaptation and fracture resistance of endocrown restorations utilizing different machinable blocks subjected to thermomechanical aging. *J Esthet Restor Dent.* 2018;30(4):319-328.
34. Nawafleh NA, Mack F, Evans J, Mackay J, Hatamleh MM. Accuracy and reliability of methods to measure marginal adaptation of crowns and FDPs: a literature review. *J Prosthodont.* 2013;22(5):419-428.
35. Donmez MB, Okutan Y. Marginal gap and fracture resistance of implant-supported 3D-printed definitive composite crowns: An in vitro study. *J Dent.* 2022;124:104216.
36. Alharbi N, Alharbi S, Cuijpers VMJI, Osman RB, Wismeijer D. Three-dimensional evaluation of marginal and internal fit of 3D-printed interim restorations fabricated on different finish line designs. *J Prosthodont Res.* 2018;62(2):218-226.
37. Kakinuma H, Izumita K, Yoda N, Egusa H, Sasaki K. Comparison of the accuracy of resin-composite crowns fabricated by three-dimensional printing and milling methods. *Dent Mater J.* 2022;41(6):808-815.
38. Godil AZ, Kazi AI, Wadwan SA, Gandhi KY, S. Dugal RJ. Comparative evaluation of marginal and internal fit of endocrowns using lithium disilicate and polyetheretherketone computer-aided design - computer-aided manufacturing (CAD-CAM) materials: An in vitro study. *J Conserv Dent* 2021;24:190-4.
39. Elsharkawy A. Marginal adaptation and fracture resistance of endocrown restorations constructed from two Cad /Cam blocks. *Egyptian Dental Journal.* 2021;67(4):3547-60.
40. Jacobs MS, Windeler AS. An investigation of dental luting cement solubility as a function of the marginal gap. *J Prosthet Dent.* 1991;65(3):436-442.
41. McLean JW, von Fraunhofer JA. The estimation of cement film thickness by an in vivo technique. *Br Dent J.* 1971;131(3):107-111.
42. Rosentritt M, Sikora M, Behr M, Handel G. In vitro fracture resistance and marginal adaptation of metallic and tooth-coloured post systems. *J Oral Rehabil.* 2004 Jul; 31(7):675-81.
43. Morresi AL, D'Amario M, Monaco A, Rengo C, Grassi FR, Capogreco M. Effects of critical thermal cycling on the flexural strength of resin composites. *J Oral Sci.* 2015;57(2):137-143.
44. Krejci I, Mueller E, Lutz F. Effects of thermocycling and occlusal force on adhesive composite crowns. *J Dent Res.* 1994;73(6):1228-1232.
45. Beschnidt SM, Strub JR. Evaluation of the marginal accuracy of different all-ceramic crown systems after simulation in the artificial mouth. *J Oral Rehabil.* 1999; 26(7):582-593.
46. Emsermann I, Eggmann F, Krastl G, Weiger R, Amato J. Influence of Pretreatment Methods on the Adhesion of Composite and Polymer Infiltrated Ceramic CAD-CAM Blocks. *J Adhes Dent.* 2019;21(5):433-443.
47. Soares CJ, Pizi EC, Fonseca RB, Martins LR. Influence of root embedment material and periodontal ligament simulation on fracture resistance tests. *Braz Oral Res.* 2005;19(1):11-16.
48. Wedekind, L.; Güth, J.F.; Schweiger, J.; Kollmuss, M.; Reichl, F.X.; Edelhoff, D.; Högg, C. Elution behavior of a 3D-printed, milled and conventional resin-based occlusal splint material. *Dent. Mater.* 2021; 37:701-710.
49. Zimmermann M, Ender A, Egli G, Özcan M, Mehl A. Fracture load of CAD/CAM-fabricated and 3D-printed composite crowns as a function of material thickness. *Clin Oral Investig.* 2019;23(6):2777-2784.
50. Bousdras VA, Cunningham JL, Ferguson-Pell M, et al. A novel approach to bite force measurements in a porcine model in vivo. *Int J Oral Maxillofac Surg.* 2006;35(7):663-667.